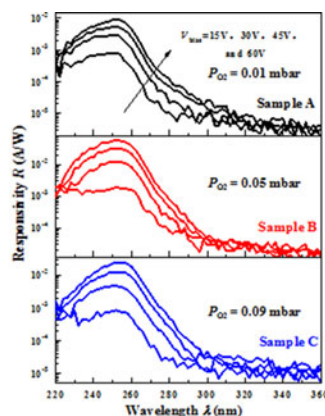
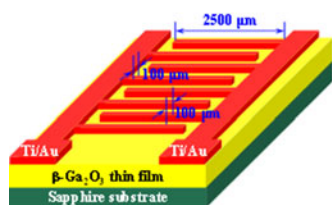


# Comparison Study of $\beta$ -Ga<sub>2</sub>O<sub>3</sub> Photodetectors Grown on Sapphire at Different Oxygen Pressures

Volume 9, Number 4, August 2017

Lu Huang  
Qian Feng  
Genquan Han, *Member, IEEE*  
Fuguo Li  
Xiang Li  
Liwei Fang  
Xiangyu Xing  
Jincheng Zhang  
Yue Hao, *Senior Member, IEEE*



DOI: 10.1109/JPHOT.2017.2731625  
1943-0655 © 2017 IEEE

# Comparison Study of $\beta$ -Ga<sub>2</sub>O<sub>3</sub> Photodetectors Grown on Sapphire at Different Oxygen Pressures

Lu Huang, Qian Feng, Genquan Han, *Member, IEEE*, Fuguo Li, Xiang Li, Liwei Fang, Xiangyu Xing, Jincheng Zhang, and Yue Hao, *Senior Member, IEEE*

State Key Discipline Laboratory of Wide Band Gap Semiconductor Technology, School of Microelectronics, Xidian University, Xi'an 710071, China

DOI:10.1109/JPHOT.2017.2731625

1943-0655 © 2017 IEEE. Translations and content mining are permitted for academic research only. Personal use is also permitted, but republication/redistribution requires IEEE permission. See [http://www.ieee.org/publications\\_standards/publications/rights/index.html](http://www.ieee.org/publications_standards/publications/rights/index.html) for more information.

Manuscript received April 18, 2017; revised July 15, 2017; accepted July 19, 2017. Date of publication June 30, 2017; date of current version August 8, 2017. This work was supported by the National Natural Science Foundation of China under Grant 61534004, Grant 61334002, and Grant 51321091. The work of Q. Feng was supported by the State Key Laboratory of Crystal Materials (Shandong University). Corresponding authors: Qian Feng, Genquan Han, and Jincheng Zhang (e-mail: qfeng@mail.xidian.edu.cn; hangenquan@ieee.org; jchzhang@xidian.edu.cn).

**Abstract:** In this paper,  $\beta$ -Ga<sub>2</sub>O<sub>3</sub> ultraviolet photodetectors were grown on sapphire utilizing the laser molecular beam epitaxy tool. The impact of oxygen pressure  $P_{O_2}$  in growth chamber on the crystal quality, the surface morphology, the chemical component of Ga<sub>2</sub>O<sub>3</sub> films, and the electrical performance of photodetectors are characterized. As the  $P_{O_2}$  is increased during growth, the concentration of oxygen vacancy ( $V_O$ ) is effectively reduced. The photodetector grown at the  $P_{O_2}$  of 0.05 mbar exhibits the significantly improved photocurrent  $I_{photo}$  and responsivity  $R$  characteristics in comparison with the device grown with the  $P_{O_2}$  of 0.01 mbar, which is attributed to a reduction in the number of  $V_O$ . However, as the  $P_{O_2}$  continuously increased to 0.09 mbar,  $I_{photo}$  and  $R$  of the detector are degraded, which might be due to the fact that the gallium vacancies ( $V_{Ga}$ ), as the dominant trapping centers, lead to the recombination of photo-generated carriers.

**Index Terms:**  $\beta$ -Ga<sub>2</sub>O<sub>3</sub>, photodetectors, oxygen pressure.

## 1. Introduction

Ultraviolet photodetectors are important devices that can be used in various civil and military applications, including solar UV monitoring, missile tracking, UV astronomy, flame sensors, and chemical/biological analysis [1], [2]. The materials with wide bandgap  $E_G$  are considered to be ideal for solar-blind photodetectors to minimize the chance of false detection. Gallium oxide (Ga<sub>2</sub>O<sub>3</sub>) is one of the promising candidates for the deep ultraviolet detection because of its 4.8–4.9 eV  $E_G$  producing high transparency at the wavelength  $\lambda$  longer than 300 nm [3] and the excellent chemical and thermal stability. Up to now, the great research efforts have been devoted to exploring the epitaxial growth of Ga<sub>2</sub>O<sub>3</sub> films by pulsed laser deposition (PLD) or laser molecular beam epitaxy (MBE) [3]–[6], metalorganic chemical vapor deposition (MOCVD) [7], solid source MBE [8], and magnetron sputtering [9] on different substrates [10]–[13]. Compared to the other epitaxial growth techniques, laser MBE has the advantages of higher purity of source materials and lower impurity levels. The Ga<sub>2</sub>O<sub>3</sub> based solar blind photodetectors have been demonstrated based on Ga<sub>2</sub>O<sub>3</sub>

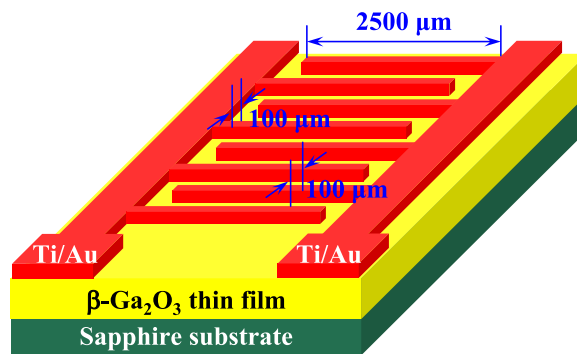


Fig. 1. The schematic of the Ga<sub>2</sub>O<sub>3</sub> photodetector.

films [14], Ga<sub>2</sub>O<sub>3</sub> nanowires [15], Ga<sub>2</sub>O<sub>3</sub> single crystals [15], and (AlGa)<sub>2</sub>O<sub>3</sub> films [16]. However, the experimental results indicated that the point defects, including oxygen vacancy  $V_O$ , interstitial oxygen atom, gallium vacancy  $V_{Ga}$ , and interstitial atom, could serve as trapping and recombination centers, which reduced the collection efficiency of the photogenerated carriers by the electrodes, therefore leading to the degradation of photocurrent  $I_{photo}$  and responsivity  $R$  [17], [18]. The process parameters during material growth directly affected the formation of point defects in Ga<sub>2</sub>O<sub>3</sub> [19], which determined the photodetector performance. The influence of growth temperature, annealing, and Sn doping on the Ga<sub>2</sub>O<sub>3</sub> photodetectors performance has been studied [3], [5], [6]. There is still a lack of the experimental study on the dependence of Ga<sub>2</sub>O<sub>3</sub> photodetector performance on the oxygen pressure  $P_{O_2}$  in the laser MBE chamber.

In this paper, we report the demonstration of Ga<sub>2</sub>O<sub>3</sub> photodetectors with  $\beta$ -Ga<sub>2</sub>O<sub>3</sub> epitaxially grown on sapphire at different oxygen pressure  $P_{O_2}$  utilizing laser MBE. The impacts of  $P_{O_2}$  in growth chamber on the stoichiometries of Ga<sub>2</sub>O<sub>3</sub> and the device performance are investigated.

## 2. Materials Characterization and Device Fabrication

The  $\beta$ -Ga<sub>2</sub>O<sub>3</sub> films were epitaxially grown on sapphire (0001) substrate using laser MBE at 600 °C with three different  $P_{O_2}$ , 0.01, 0.05, and 0.09 mbar, denoted as sample A, B, and C, respectively. The cylindrical Ga<sub>2</sub>O<sub>3</sub> ceramic target (99.99% purity) was irradiated by the KrF excimer laser beam with the laser energy density of 2 J/cm<sup>2</sup> at the repetition rate of 5 Hz and the distance between the sapphire substrate and Ga<sub>2</sub>O<sub>3</sub> target was fixed at 5 cm. The base pressure of the growth chamber was  $1.5 \times 10^{-8}$  Torr. Photodetectors with interdigital Ti/Au (20 nm/100 nm) contacts were fabricated on the  $\beta$ -Ga<sub>2</sub>O<sub>3</sub> films. The electrode fingers were 100  $\mu$ m wide and 2500  $\mu$ m long with a 100  $\mu$ m spacing gap. Fig. 1 shows the schematic diagram of the fabricated device.

The crystal structure and orientation of Ga<sub>2</sub>O<sub>3</sub> samples were studied by the high-resolution X-ray diffraction (HRXRD). The surface morphology was investigated with atomic force microscope (AFM) with Agilent 5500 in tapping mode. The stoichiometries of Ga<sub>2</sub>O<sub>3</sub> samples were analyzed with X-ray photoelectron spectroscopy (XPS). Characterization of  $I_{photo}$ ,  $R$ , time-dependent photoresponse, and the dark current  $I_{dark}$  of the Ga<sub>2</sub>O<sub>3</sub> photodetectors were carried out utilizing a low-pressure mercury lamp U3900 with the illumination  $\lambda$  from 254 to 365 nm and the various power densities  $P_{light}$ . The illumination  $\lambda$  on the devices was measured using the optical grating.

## 3. Results and Discussion

### 3.1 Material Characterization

Fig. 2 presents the HRXRD curves of the Ga<sub>2</sub>O<sub>3</sub> films grown with different  $P_{O_2}$  on sapphire. Three diffraction peaks corresponding to  $\beta$ -Ga<sub>2</sub>O<sub>3</sub> (201), (402), and (603) planes are observed, which indicates the single crystallinity of the  $\beta$ -Ga<sub>2</sub>O<sub>3</sub> phase. Fig. 3 shows the surface morphologies of

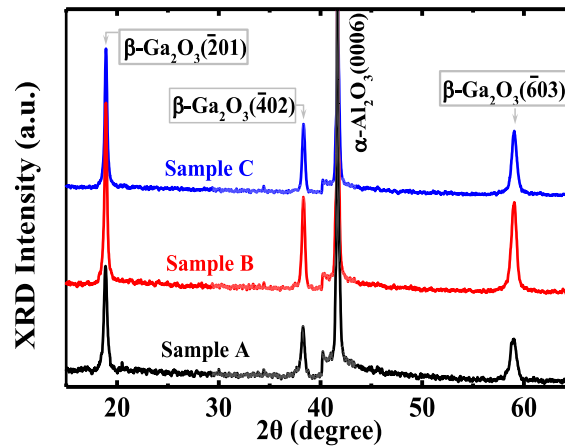


Fig. 2. HRXRD diffraction curves of the Ga<sub>2</sub>O<sub>3</sub> samples on sapphire.

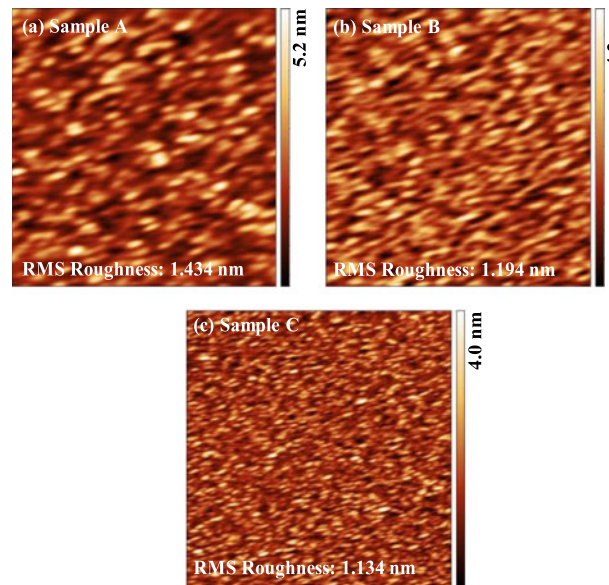


Fig. 3. AFM images of Ga<sub>2</sub>O<sub>3</sub>. (a) Sample A, (b) Sample B, and (c) Sample C.

the  $\beta$ -Ga<sub>2</sub>O<sub>3</sub> samples measured by AFM with a scanning area of  $5\ \mu\text{m} \times 5\ \mu\text{m}$ . The values of the root-mean-square (RMS) roughness of Sample A, B, and C are 1.434, 1.194, and 1.134 nm, respectively. With the increasing  $P_{\text{O}_2}$  during the growth, the mobility of adatoms on the surface of substrate decreases, which might reduce the surface roughness of the Ga<sub>2</sub>O<sub>3</sub> film [20].

The O1s and Ga2p<sub>3/2</sub> core level XPS spectra are shown in Fig. 4. Before measurement, the *in-situ* Ar plasma etching was performed to remove the surface layer of a few nanometers and the peaks were calibrated by the adventitious C1s of 284.6 eV. The O1s peaks can be deconvoluted into three distinct peaks associated with Ga<sub>2</sub>O<sub>3</sub>, oxygen vacancy, and the assorted gallium suboxides of Ga<sub>2</sub>O and GaO. Taken into account both the sensitivity factor and the area of peaks, the ratio of O/Ga in three Ga<sub>2</sub>O<sub>3</sub> samples is 1.03, 1.08, and 1.09, respectively. The O1s binding energy has a shift toward the higher binding energy with the increasing of  $P_{\text{O}_2}$ , which is indicative of the increasing in the number of oxygen atoms, i.e., the reduction in the concentration of  $V_{\text{O}}$  [21]. The Ga2p<sub>3/2</sub> peaks can also be deconvoluted into two distinct peaks associated with Ga<sub>2</sub>O<sub>3</sub> and the gallium suboxides. What's more, the Ga2p<sub>3/2</sub> peaks also shift to the higher binding energy, which is due to the increasing of Ga-O binding structure [21].

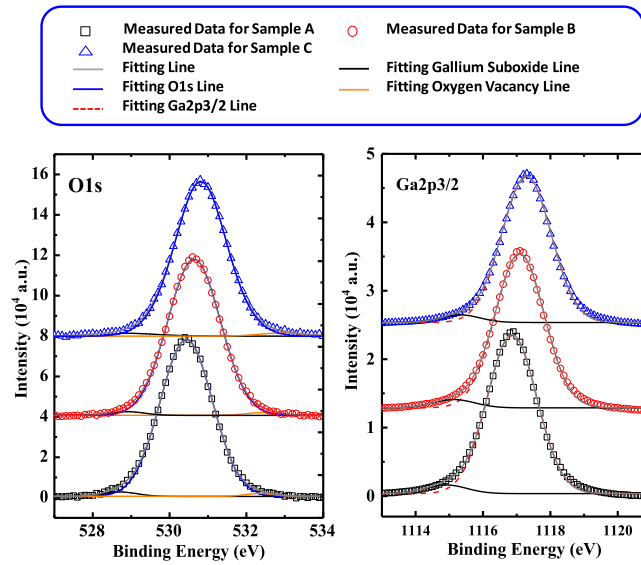


Fig. 4. XPS spectra of O1s and Ga2p3/2 core level of the Ga<sub>2</sub>O<sub>3</sub> samples.

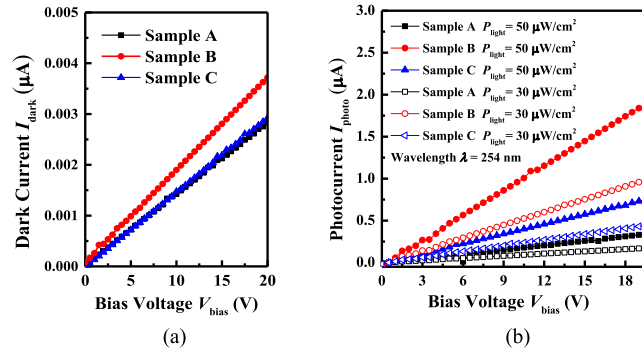


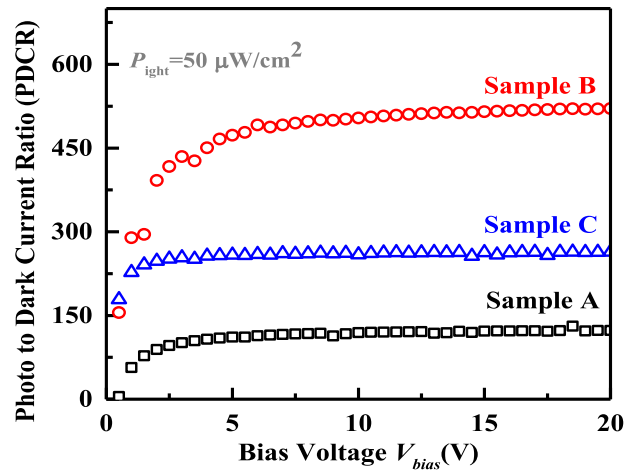
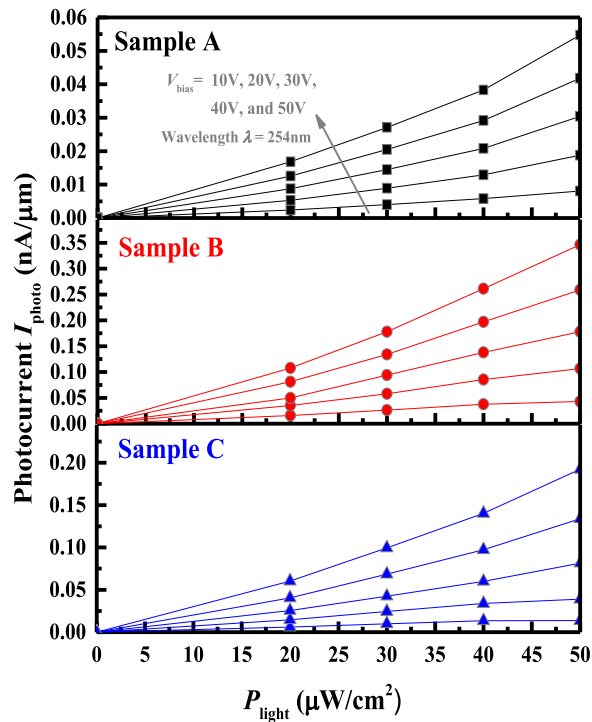
Fig. 5. (a)  $I_{\text{dark}}$  and (b)  $I_{\text{photo}}$  versus  $V_{\text{bias}}$  characteristics for the Ga<sub>2</sub>O<sub>3</sub> photodetectors.

### 3.2 Electrical Characteristics of the Devices

The  $I_{\text{dark}} - V_{\text{bias}}$  and  $I_{\text{photo}} - V_{\text{bias}}$  curves for the photodetectors under various  $P_{\text{light}}$  are depicted in Fig. 5.  $I_{\text{photo}}$  and  $I_{\text{dark}}$  of devices have the obvious relation to the  $P_{\text{light}}$ . Compared with the other two samples, the Sample B obtains a higher  $I_{\text{dark}}$  and  $I_{\text{photo}}$ . It is speculated that the Sample B has fewer  $V_{\text{O}}$  than the Sample A, owing to the higher  $P_{\text{O}_2}$  during growth. For the growth of Sample C, the even higher  $P_{\text{O}_2}$  might produce a large number of  $V_{\text{Ga}}$  and  $V_{\text{O}} - V_{\text{Ga}}$  complexes [22]. The point defects, whether  $V_{\text{O}}$ ,  $V_{\text{Ga}}$  and  $V_{\text{O}} - V_{\text{Ga}}$ , can act as trapping centers to capture the photo-generated carriers, leading to the degradation of  $I_{\text{photo}}$  of the devices.

As illustrated in Fig. 6, the Sample B demonstrates a photo to dark current ratio (PDCR) of 510, which is much higher than those of the other two samples, less than 300. Thus, it is considered that, compared to Samples A and C, Sample B has a much smaller number of such points defects acting as trapping centers to capture the photo-generated carriers. Fig. 7 shows the superlinear  $I_{\text{photo}}$  as a function of  $P_{\text{light}}$  at different bias voltage  $V_{\text{bias}}$  for the devices, indicating the optical gain of the three photodetectors. This is due to the channel resistance reduction resulted from the increasing of photo-generated carriers and the decreasing of the effective barrier height for electrons at the ground contact caused by the accumulation of holes at the Ga<sub>2</sub>O<sub>3</sub>/metal junction [23].

Fig. 8 shows the  $R$  as a function of  $\lambda$  of the illumination light for the Ga<sub>2</sub>O<sub>3</sub> detectors. Solar-blind operation was obtained for all the three samples with the excellent solar rejection ratio for  $\lambda$  larger than 300 nm and the strong photoconductive gain for  $\lambda$  smaller than 280 nm. The Sample

Fig. 6. PDCR of the  $\beta$ -Ga<sub>2</sub>O<sub>3</sub> photodetectors.Fig. 7. Superlinear  $I_{\text{photo}}$  as a function of  $P_{\text{light}}$  of the devices.

B achieves the improved  $R$  compared to the others. At a  $V_{\text{bias}}$  of 60 V, the maximum  $R$ ,  $R_{\text{max}}$ , of 0.009, 0.058, and 0.025 A/W are obtained in the Sample A, B, and C, respectively. The values of external quantum efficiency (EQE), calculated by  $\text{EQE} = hcR_{\text{max}}/(e\lambda)$ , are 4.39%, 28.3%, and 12.2% for the Sample A, B, and C, respectively. Here,  $h$  is Planck's constant,  $c$  is the velocity of light,  $e$  is the electronic charge, and  $\lambda$  is the incident light  $\lambda$ . The value of cutoff  $\lambda$  of Ga<sub>2</sub>O<sub>3</sub> devices, defined as the  $\lambda$  at  $\sqrt{1/2R_{\text{max}}}$  is about 259 nm, indicating the  $E_{\text{G}}$  of 4.79 eV. We compare the  $I_{\text{dark}}$ ,  $I_{\text{photo}}$ , PDCR,  $R_{\text{max}}$ , and EQE characteristics of the devices in Table 1, showing that sample B has the improved performance compared to the other two. The sample B also demonstrates the higher PDCR compared to devices in Refs. [3] and [6]. In Ref. [5], heterostructure was used to further enhance the device performance.



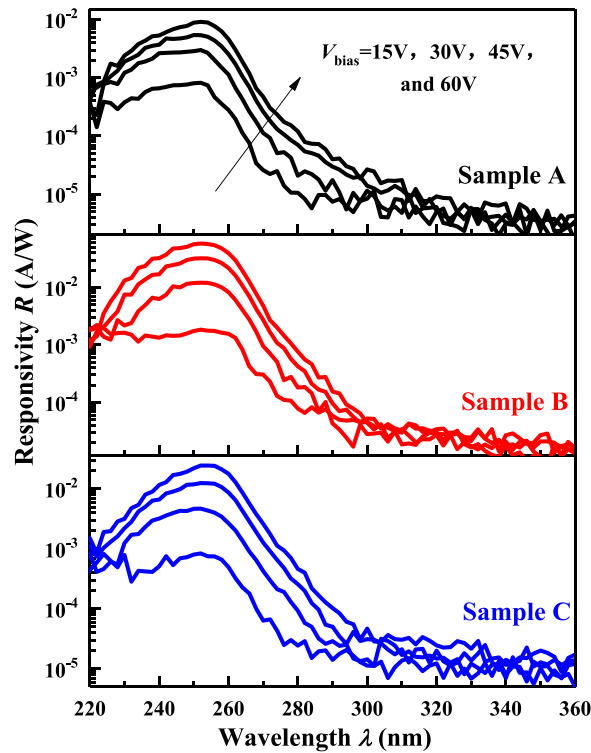


Fig. 8. Responsivity versus illumination optical  $\lambda$  for the Ga<sub>2</sub>O<sub>3</sub> photodetectors at various  $V_{\text{bias}}$ .

TABLE 1  
Comparison of the Electrical Performance of the Photodetectors

	$I_{\text{dark}} @ 10 \text{ V (nA)}$	$I_{\text{photo}} @ 10 \text{ V } (\mu\text{A})$	PDCR @ 10 V	$R_{\text{max}} \text{ (A/W)}$	EQE
Sample A	1.4	0.17	119	0.01	4.39%
Sample B	1.9	1.00	504	0.06	28.3%
Sample C	1.5	0.38	259	0.03	12.2%

Fig. 9 presents the transient response curves of the Ga<sub>2</sub>O<sub>3</sub> photodetectors on sapphire. Measurements of the time-dependent photoresponse characteristics were carried out utilizing a 254 nm square-wave light with a period of 6 s under a  $P_{\text{light}}$  of 20  $\mu\text{W}/\text{cm}^2$  and a  $V_{\text{bias}}$  of 10 V. In all devices, we can find two different relaxation durations in the rise and decay processes: the fast-response and the slow-response. Table 2 lists the values of the rise time constants ( $\tau_{r1}$  and  $\tau_{r2}$ ) and those of the decay time ( $\tau_{d1}$  and  $\tau_{d2}$ ). The fast responses,  $\tau_{r1}$  and  $\tau_{d1}$ , are related to the direct band to band transition, and the slow response during the rise process might be associated with the transition between band edge and defects bands. The slow response in the decay process could be ascribed to the recombination of the carriers trapped by the trapping center through the defects bands, thus resulting in the obvious persistent photoconductivity (PPC) phenomenon.

It was reported that  $V_{\text{O}}$ , having the lower formation energy under O-poor (or Ga-Rich) condition, acts as the deep donor [24], [25]. Some studies showed that  $V_{\text{O}}$  interacted with  $V_{\text{Ga}}$  to form  $V_{\text{O}} - V_{\text{Ga}}$  compounds, acting as the acceptors [26]–[30]. For Ga<sub>2</sub>O<sub>3</sub> grown under a  $P_{\text{O}_2}$  of

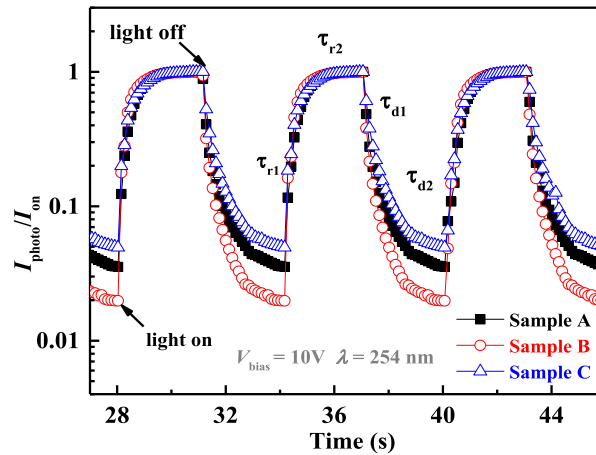


Fig. 9. Time-dependent photoresponse characteristics of the Ga<sub>2</sub>O<sub>3</sub> photodetectors on sapphire.

TABLE 2

The Rise Time Constants ( $\tau_{r1}$  and  $\tau_{r2}$ ) and Values of Decay Time ( $\tau_{d1}$  and  $\tau_{d2}$ )

	$\tau_{r1}$	$\tau_{r2}$	$\tau_{d1}$	$\tau_{d2}$
Sample A	0.46 s	2.55 s	0.23 s	2.78 s
Sample B	0.47 s	2.45 s	0.28 s	2.69 s
Sample C	0.45 s	2.55 s	0.23 s	2.78 s

0.01 mbar, the generated  $V_O$  could trap photo-generated carriers, leading to the slower response in the decay process. As  $P_{O_2}$  rising, the oxygen concentration in the epitaxial Ga<sub>2</sub>O<sub>3</sub> increases and the concentration of  $V_O$  decreases, and thus the value of  $\tau_{d2}$  in Sample B is reduced compared to Sample A. For the sample grown under a  $P_{O_2}$  of 0.09 mbar, although the generation of  $V_O$  is further suppressed, other point defects, such as  $V_{Ga}$  and  $V_O - V_{Ga}$  might be the dominant trapping centers to trap carriers during illumination [28], [30], so the  $\tau_{d2}$  becomes larger again in Sample C.

#### 4. Conclusion

The  $\beta$ -Ga<sub>2</sub>O<sub>3</sub> photodetectors were grown on sapphire (0001) substrate at the different  $P_{O_2}$  by laser MBE. Compared to Sample A and C, Sample B achieves the improved  $I_{photo}$ ,  $R$ , and time-dependent photoresponse characteristics. It is speculated the  $P_{O_2}$  has a great impact on the formation of  $V_O$  and  $V_{Ga}$  defects. Sample A might contain more  $V_O$  than Sample B due to the lower  $P_{O_2}$  during growth, resulting in the reduced  $I_{photo}$ , and for the Sample C, the  $P_{O_2}$  is much higher in comparison Sample B, which could lead to the formation of a large number of  $V_{Ga}$ , lowering the  $I_{photo}$ .

#### Acknowledgment

The authors would like to acknowledge Prof. Dabing Li from Changchun Institute of Optics, Fine Mechanical and Physics, Chinese Academy of Sciences for the responsivity measurements.



## References

- [1] P. Feng, J. Y. Zhang, Q. H. Li, and T. H. Wang, "Individual  $\beta$ -Ga<sub>2</sub>O<sub>3</sub> nanowires as solar-blind photodetectors," *Appl. Phys. Lett.*, vol. 88, no. 15, Mar. 2006, Art. no. 153107.
- [2] R. Suzuki, S. Nakagomi, and Y. Kokubun, "Solar-blind photodiodes composed of an Au Schottky contact and a  $\beta$ -Ga<sub>2</sub>O<sub>3</sub> single crystal with a high resistivity cap layer," *Appl. Phys. Lett.*, vol. 98, no. 13, Mar. 2011, Art. no. 131114.
- [3] D. Y. Guo *et al.*, "Fabrication of  $\beta$ -Ga<sub>2</sub>O<sub>3</sub> thin films and solar-blind photodetector by laser MBE technology," *Opt. Mater. Exp.*, vol. 4, no. 5, pp. 1067–1076, May 2014.
- [4] A. Pettimangin *et al.*, "Characterization of oxygen deficient gallium oxide films grown by PLD," *Appl. Surf. Sci.*, vol. 278, no. 8, pp. 153–157, Aug. 2013.
- [5] Y. H. An, D. Y. Guo, S. Y. Li, Z. P. Wu, and Y. Q. Huang, "Influence of oxygen vacancies on the photoresponse of  $\beta$ -Ga<sub>2</sub>O<sub>3</sub>/SiC n–n type heterojunctions," *J. Phy. D, Appl. Phys.*, vol. 49, no. 28, 2016, Art. no. 285111.
- [6] X. Zhao *et al.*, "Growth and characterization of Sn doped  $\beta$ -Ga<sub>2</sub>O<sub>3</sub> thin films and enhanced performance in a solar-blind photodetector," *J. Electron. Mater.*, vol. 46, no. 6, pp. 2366–2372, 2017.
- [7] G. Wagner *et al.*, "Homoepitaxial growth of  $\beta$ -Ga<sub>2</sub>O<sub>3</sub> layers by metal-organic vapor phase epitaxy," *Phys. Status Solidi A*, vol. 211, no. 1, pp. 27–33, Jan. 2014.
- [8] T. Oshima, N. Arai, N. Suzuki, S. Ohira, and S. Fujita, "Surface morphology of homo-epitaxial  $\beta$ -Ga<sub>2</sub>O<sub>3</sub> thin films grown by molecular beam epitaxy," *Thin Solid Films*, vol. 516, no. 17, pp. 5768–5771, Jul. 2008.
- [9] M. Ogita, K. Higo, Y. Nakanishi, and Y. Hatanaka, "Ga<sub>2</sub>O<sub>3</sub> thin film for oxygen sensor at high temperature," *Appl. Surf. Sci.*, vol. 175–176, no. 1, pp. 721–725, May 2001.
- [10] F. B. Zhang, K. Saito, T. Tanaka, M. Nishio, and Q. X. Guo, "Structural and optical properties of Ga<sub>2</sub>O<sub>3</sub> films on sapphire substrates by pulsed laser deposition," *J. Cryst. Growth*, vol. 387, pp. 96–100, Feb. 2014.
- [11] L. Y. Kong, J. Ma, C. N. Luan, W. Mi, and Y. Lv, "Structural and optical properties of hetero epitaxial beta Ga<sub>2</sub>O<sub>3</sub> films grown on MgO (100) substrates," *Thin Solid Films*, vol. 520, no. 13, pp. 4270–4274, Apr. 2012.
- [12] W. Mi, J. Ma, C. N. Luan, and H. D. Xiao, "Structural and optical properties of  $\beta$ -Ga<sub>2</sub>O<sub>3</sub> films deposited on MgAl<sub>2</sub>O<sub>4</sub>(100) substrates by metal-organic chemical vapor deposition," *J. Lumin.*, vol. 146, pp. 1–5, Feb. 2014.
- [13] V. Gottschalch *et al.*, "Growth of  $\beta$ -Ga<sub>2</sub>O<sub>3</sub> on Al<sub>2</sub>O<sub>3</sub> and GaAs using metal-organic vapor phase epitaxy," *Phys. Status Solidi A*, vol. 206, no. 2, pp. 243–249, Feb. 2009.
- [14] T. Oshima, T. Okuno, and S. Fujita, "Ga<sub>2</sub>O<sub>3</sub> thin film growth on c-plane sapphire substrates by molecular beam epitaxy for deep-ultraviolet photodetectors," *Jpn. J. Appl. Phys.*, vol. 46, pt. 1, no. 11, pp. 7217–7220, Nov. 2007.
- [15] T. Oshima, T. Okuno, N. Arai, N. Suzuki, S. Ohira, and S. Fujita, "Vertical solar-blind deep-ultraviolet Schottky photodetectors based on  $\beta$ -Ga<sub>2</sub>O<sub>3</sub> substrates," *Appl. Phys. Exp.*, vol. 1, no. 1, Jan. 2008, Art. no. 011202.
- [16] Q. Feng *et al.*, "(AlGa)<sub>2</sub>O<sub>3</sub> solar-blind photodetectors on sapphire with wider bandgap and improved responsivity," *Opt. Mater. Exp.*, vol. 7, no. 4, pp. 1240–1248, 2017.
- [17] S. C. Vanitkumari and K. K. Nanda, "A one-step method for the growth of Ga<sub>2</sub>O<sub>3</sub>-nanorod-based white-light-emitting phosphors," *J. Adv. Mater.*, vol. 21, no. 35, pp. 3581–3584, May 2009.
- [18] T. Wang and P. V. Radovanovic, "In situ enhancement of the blue photoluminescence of colloidal Ga<sub>2</sub>O<sub>3</sub> nanocrystals by promotion of defect formation in reducing conditions," *J. Chem. Commun.*, vol. 45, no. 25, pp. 7161–7163, May 2011.
- [19] T. Onuma, S. Fujioka, T. Yamaguchi, M. Higashiwaki, and K. Sasaki, "Correlation between blue luminescence intensity and resistivity in  $\beta$ -Ga<sub>2</sub>O<sub>3</sub> single crystals," *Appl. Phys. Lett.*, vol. 103, no. 4, Jul. 2013, Art. no. 041910.
- [20] Q. Feng, F. Li, B. Dai, and Z. Jia, "The properties of gallium oxide thin film grown by pulsed laser deposition," *Appl. Surf. Sci.*, vol. 359, no. 3, pp. 847–852, Dec. 2015.
- [21] S. L. Ou *et al.*, "Growth and etching characteristics of gallium oxide thin films by pulsed laser deposition," *Mater. Chem. Phys.*, vol. 133, no. 2–3, pp. 700–705, Apr. 2012.
- [22] A. M. Armstrong, M. H. Crawford, A. Jayawardena, A. Ahji, and S. Dhar, "Role of self-trapped holes in the photoconductive gain of  $\beta$ -gallium oxide Schottky diodes," *J. Appl. Phys.*, vol. 119, no. 10, Feb. 2016, Art. no. 011202.
- [23] Q. Feng *et al.*, "Comparison study of  $\beta$ -Ga<sub>2</sub>O<sub>3</sub> photodetectors on bulk substrate and sapphire," *IEEE Trans. Electron Devices*, vol. 63, no. 9, pp. 3578–3583, Sep. 2016.
- [24] J. B. Varley, J. R. Weber, A. Janotti, and C. G. Van de Walle, "Oxygen vacancies and donor impurities in  $\beta$ -Ga<sub>2</sub>O<sub>3</sub>," *Appl. Phys. Lett.*, vol. 97, no. 7, Sep. 2010, Art. no. 142106.
- [25] K. Irmscher, Z. Galazka, M. Pietsch, R. Uecker, and R. Fornari, "Electrical properties of  $\beta$ -Ga<sub>2</sub>O<sub>3</sub> single crystals grown by the Czochralski method," *J. Appl. Phys.*, vol. 110, no. 6, Aug. 2011, Art. no. 063720.
- [26] T. Harwig and F. Kellendonk, "Some observations on the photoluminescence of doped  $\beta$ -gallium sesquioxide," *J. Solid State Chem.*, vol. 24, no. 3–4, pp. 255–263, Apr. 1978.
- [27] M. C. Quinlan, M. J. O'Donnell, L. Binet, and D. Gourier, "Origin of the blue luminescence of  $\beta$ -Ga<sub>2</sub>O<sub>3</sub>," *J. Phys. Chem. Solids*, vol. 59, no. 8, pp. 1241–1249, 1998.
- [28] M. A. Blanco, M. B. Sahariah, H. Jiang, A. Costales, and R. Pandey, "Energetics and migration of point defects in Ga<sub>2</sub>O<sub>3</sub>," *Phys. Rev. B*, vol. 72, no. 18, Nov. 2005, Art. no. 184103.
- [29] T. C. Lovejoy, R. Chen, X. Zheng, E. G. Villora, and K. Shimamura, "Band bending and surface defects in  $\beta$ -Ga<sub>2</sub>O<sub>3</sub>," *Appl. Phys. Lett.*, vol. 100, no. 18, Apr. 2012, Art. no. 181602.
- [30] E. Korhonen *et al.*, "Electrical compensation by Ga vacancies in Ga<sub>2</sub>O<sub>3</sub> thin films," *Appl. Phys. Lett.*, vol. 106, no. 24, Jun. 2015, Art. no. 242103.